CHAPTER 4

DEVELOPMENT OF A 3D-PRINTED 4*F* MICROSCOPIC IMAGING PLATFORM ON SMARTPHONE

This chapter discusses in detail the realization of an affordable, and portable 4f microscopic imaging platform using a smartphone and off-the-shelf optical and electronic components. The goal of this present work is to achieve a high magnification along with micron scale optical resolution without sacrificing its FoV. In the first part of the chapter, the development of a high magnification and resolution BF smartphone microscope has been discussed. It also discusses the implementation of a cloud-based image processing algorithm to enhance further the acquired data images within the smartphone itself. In the second part of the chapter, the optimization of the 4f optical imaging configuration for fluorescence imaging has been discussed. It explains the applications of the imaging system for in-field morphological and fluorescence studies. At the end, the chapter discusses the implication of the platforms for onsite cell sorting and counting applications by using do-it-yourself (DIY) chip and custom-coded application.

4.1 Background

Due to the wide availability and accessibility even in low and middle-income countries, the smartphone has been exploited extensively for various purposes like mobile health monitoring, environmental parameters analysis etc.[1–3], which have already been brought into focus in the previous chapters. It is an ideal platform for this motive as it is embedded with many useful sensors such as the CMOS imaging sensor, ALS, gyroscopic sensor etc., along with computational units and various user-

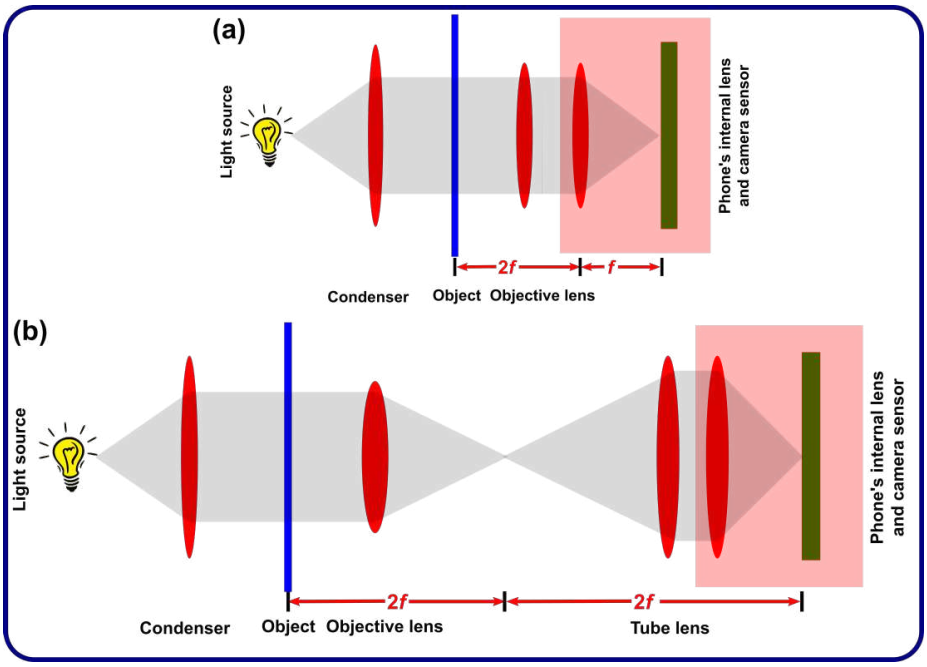

Figure 4.1: Two possible microscopic configurations on smartphone. (a) Optical setup of a $3f$ imaging system, (b) $4f$ optical imaging setup where Fourier-optics is employed to predict the behavior of the system.

friendly applications. By using 3D-printing technology, a compact optical setup can be designed to couple it to the phone, thus transforming it into a convenient and cost-effective solution for sensing and imaging applications. Again, by using custom-designed applications, it is possible to convert the designed smartphone platform tool into a standalone system that converts the results into a readable format, thus enabling a common citizen to operate the system without having technical knowledge [4]. Several low-cost, portable microscopic imaging techniques have been reported using smartphones for clinical diagnosis and other monitoring applications such as cell sorting and counting [5–7]. However, most of the phone-based microscopes use a singlet lens such as aspheric singlet, ball lens, polymer lens etc., that have very short focal length and provide pixel-limited resolution rather than diffraction-limited resolution. This means the resolution is fully dependent on the pixel pitch of the imaging sensor of the phone due to the low optical magnification of the microscopic system. Besides, the usable FoV is limited due to the aberrations and distortions of the imaging system. A fairly high magnification along with a good degree of resolution is often necessary to visualize and conduct morphological studies of biological samples such as bacteria, pathogens, blood cells etc.. Thus, there are immense scopes for optimization in the optical designing of such low-cost imaging systems.

There are two possible methods to realize microscopic setup, so-called $3f$ and $4f$ imaging systems on a smartphone, as shown in figure 4.1. The $3f$ configuration, shown in figure 4.1(a), allows a very simple and compact implementation of the optical

imaging setup. Here, simply an external lens is mounted directly to the smartphone camera sensor-lens module to form a finite-conjugate system. The built-in camera lens of the phone will work as a tube lens in the optical configuration. This setup of an imaging system is simple and offers the highest acceptance for red and blue light than its $4f$ counterpart [8]. However, the focal length of the external lens should be very small to achieve an acceptable magnification of 1 ($M \geq 1$). The development of this imaging configuration has already been thoroughly discussed in the chapter 3. On the contrary, the implementation of the $4f$ configuration, shown in figure 4.1(b), is a bit complex and requires more number of good quality optics. This increases the overall cost and size of the imaging system in comparison to a $3f$ imaging setup. Here, the objective lens and tube lens are stacked adjacently such that their focal planes coincide to realize tele-centricity. This allows to limit the optical aberrations in the imaging system, and the behavior of the system is determined using Fourier-optics [9, 10]. Modern optical microscopes that are based on infinity-corrected objectives often follow this configuration. The use of $4f$ imaging configuration enables the designed platform to perform at its highest potential by fully utilizing the NA of the objective lens. This chapter decodes the realization of the inexpensive, robust and user-friendly smartphone-based microscopic platforms implementing the $4f$ optical configuration for various applications from morphological study to onsite cell counting.

4.2 Design of a field-portable, inexpensive smartphone microscopic system for biomedical applications

Portable, low-cost smartphone platform microscopic system has already emerged as a potential tool for imaging various micron and sub-micron scale particles in recent years [5]. Most of the reported works involve either the use of sophisticated optical setups along with a high-end computational tool for post-processing of the captured images or require a high-end configured smartphone to obtain enhanced imaging of the sample. This section of the chapter discusses the working of a low-cost, field-portable 520× optical microscope using a smartphone. The proposed microscopic system works on the principle of a $4f$ imaging system. The proposed system has been obtained by attaching a 3D printed compact optical setup to the rear camera of a smartphone. By using cloud-based services, an image processing algorithm has been developed, which can be accessed anytime through a mobile broadband network. Using this facility, the quality of the captured images can be enhanced further, thus obviating the need for dedicated computational tools for the post-processing of the

Figure 4.2: Schematic illustration of the working steps of the proposed optical microscope.

images. This section intends to manifest that with a properly designed optical setup in a 3D printer and by developing an image processing application in the cloud, it is possible to obtain a low-cost, user-friendly, field-portable optical microscope on a regular smartphone that performs at par with that of a laboratory-grade microscope. Figure 4.2 shows the process flow of the proposed smartphone optical microscopic system.

4.2.1 Working Principle and device construction

Design, fabrication and assembly

To develop the proposed smartphone-based optical microscope, a pair of ball lenses (diameter 1 mm, from Edmund Optics Inc., Barrington, USA, Part no. #43708) and plano-convex lens (focal length 11 mm, 6 mm diameter, from Holmarc Opto-Mechatronics, India) has been used as magnifying optics. The combination of these two lenses provides an optical magnification of 520×. For the illumination of the specimen, an external white LED (Robomart, India, Part no. RM0803) has been used as an optical source. The LED is powered from the smartphone battery through the USB-OTG protocol. The emitting light from the LED is collimated by a double-convex lens and then diffused by allowing it to pass through a diffuser. This ensures

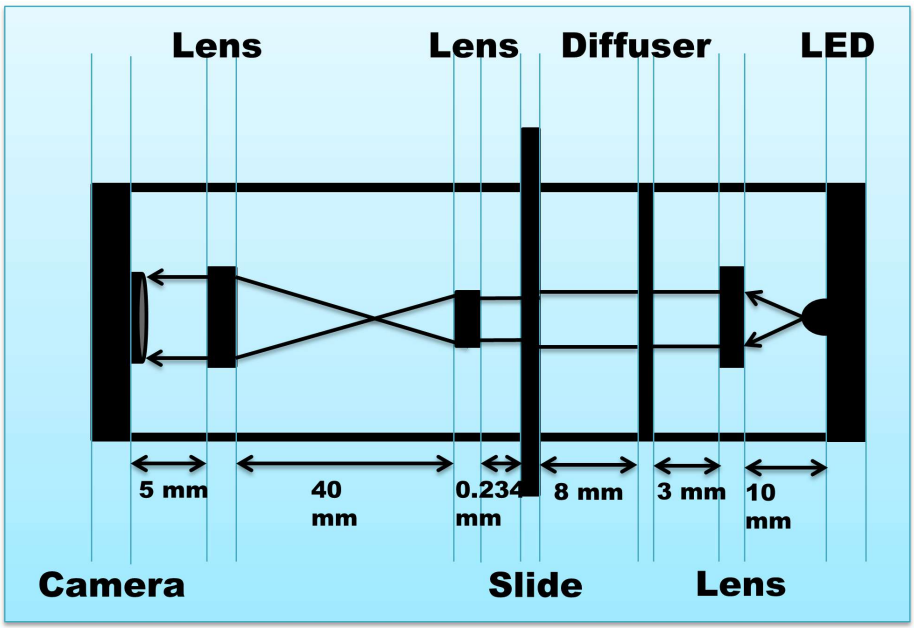

Figure 4.3: Optimized optical design of the proposed smartphone microscopic imaging system.

a uniform illumination over the imaging region of the specimen. The schematic of the proposed optical configuration is shown in figure 4.3. The performance of the optical design has been optimized by eliminating the peripheral rays from the edges of the FoV by introducing an aperture stop just before the ball lens. This would restrict the defocus rays to pass through the ball lens, and thus possible spherical aberration and distortions in the final image have been minimized. The required optics design for the proposed smartphone microscope has been carried out by approximating the paraxial model in Zeemax Optic Studio software. This is illustrated in figure 4.4. It was observed that the reasonable modulation transfer function (MTF) of the proposed system is 825 cycles/mm. This corresponds to a resolution of 1.2 μm at the object plane.

The proposed optical setup has been designed using ZW3D - licensed CAD software and for controlling of the layer resolution of the setup, a freely available software- 'Ideamaker slicing engine' from Raise3D has been used. The plastic optical setup has been fabricated using an FDM 3D printer (Raise3D model N2). This specific 3D printer has a nozzle diameter of 400 μm with a maximum layer resolution of 10 μm having position accuracy of 1.25 μm in Z-direction and 1.25 μm X/Y step size. In the present work, PLA polymer filament has been used for the printing of the opto-mechanical parts. Figure 4.5(A) shows the schematic of the proposed smartphone microscopic system. The designed opto-mechanical system houses all the required optical components which can be coupled easily to the rear camera of the smartphone. Figure 4.5(B) shows the photo image of the designed smartphone microscope. In the present work, Moto G5 Plus (XT1686 from Motorola Inc.) smartphone has

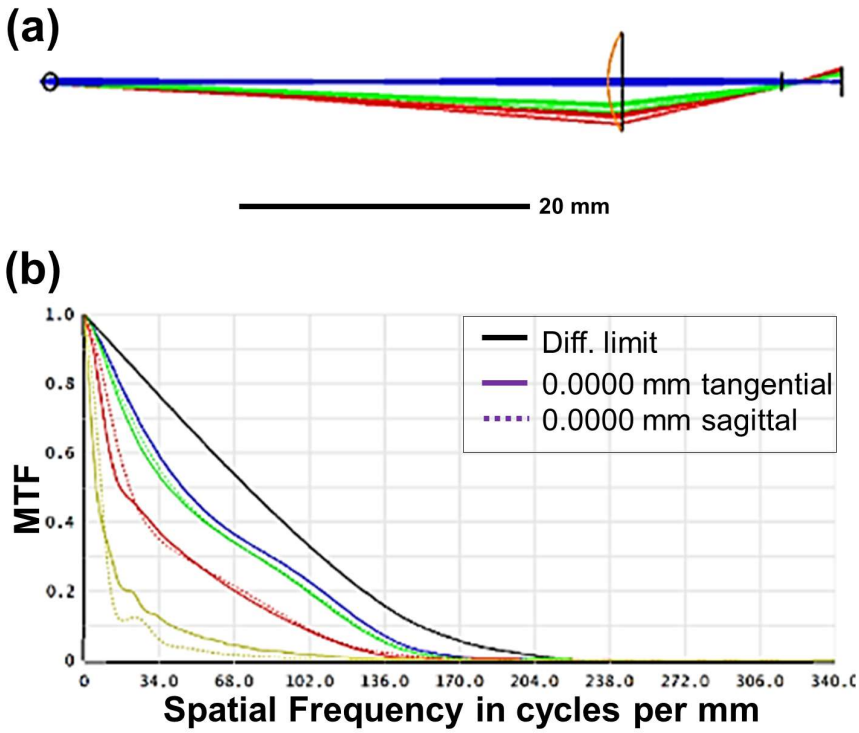

Figure 4.4: Ray tracing simulation of the optical schemes. (a) Zeemax model of the proposed smartphone microscope, and (b) its MTF at the object plane.

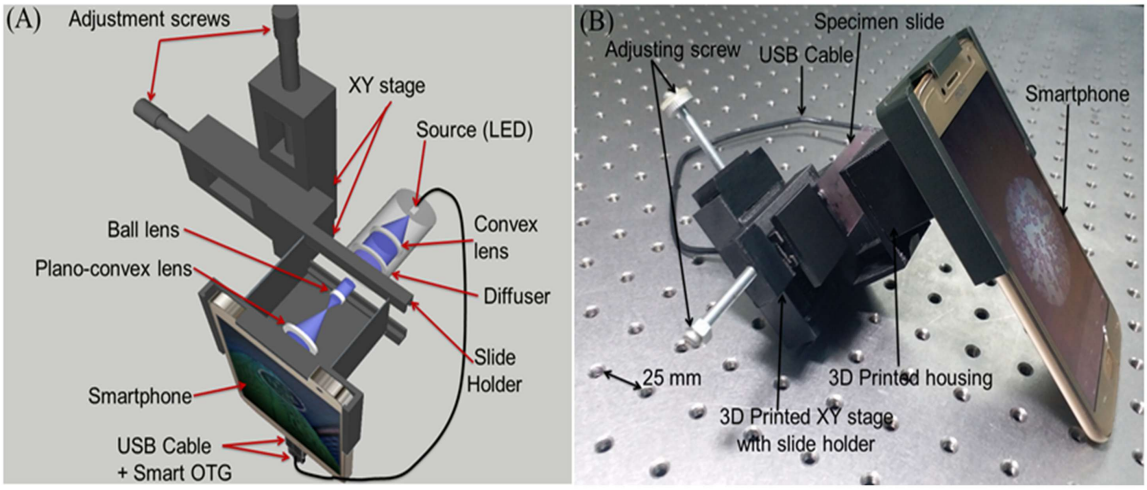

Figure 4.5: Smartphone based microscope: (A) the optical layout, (B) the 3D printed prototype installed on an android smartphone device.

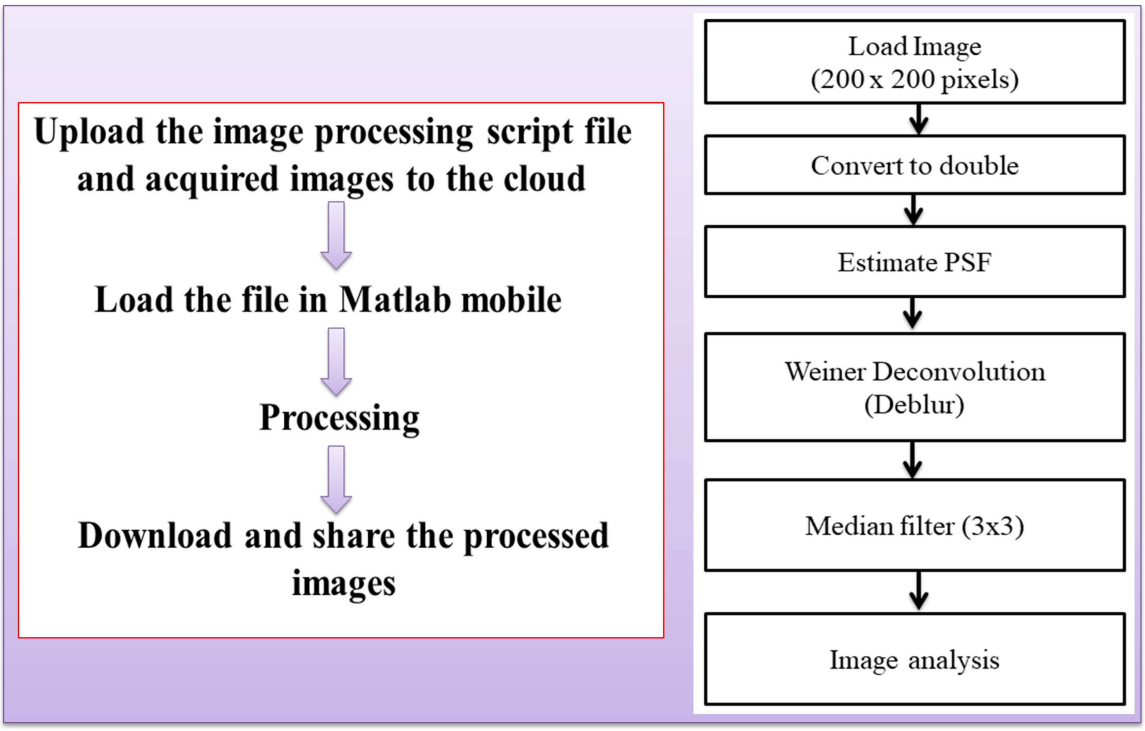

Figure 4.6: Development of an image processing algorithm to enhance the captured images using Matlab mobile application.

been used to capture the microscopic images. Owing to its affordable price, Moto G5 Plus is one of the most commonly used smartphones in India. This phone is equipped with a Qualcomm Snapdragon processor with 4 GB Random Access Memory (RAM) with a storage capacity of 32 GB. The 12.2 MP rear camera of the phone is embedded with CMOS imaging sensor having a pixel size of 1.4 μm and is attached with an $f/1.7$ aperture lens.

4.2.2 Development of applications in cloud server

To run an image processing application, usually it needs a high-speed processor along with a high configured RAM (6 GB or more), and a regular smartphone may lack these features for the processing of an image within the phone itself. In this section, for the development of image processing algorithm, the cloud-based 'Matlab mobile' platform has been used. All the image processing functions can be accessed easily from the cloud for development of the custom-designed application. The designed algorithm can be uploaded in the cloud, and the same can be accessed through Matlab mobile application on a smartphone from anywhere in the world. This is shown in figure 4.6. To process the captured images by the designed microscopic system, two functions were mainly used from Matlab library-Weiner deconvolution followed by the use of median filter. Here, the Weiner deconvolution function (*deconvwnr*) with an estimated point-spread-function (PSF) has been used to deblur the original

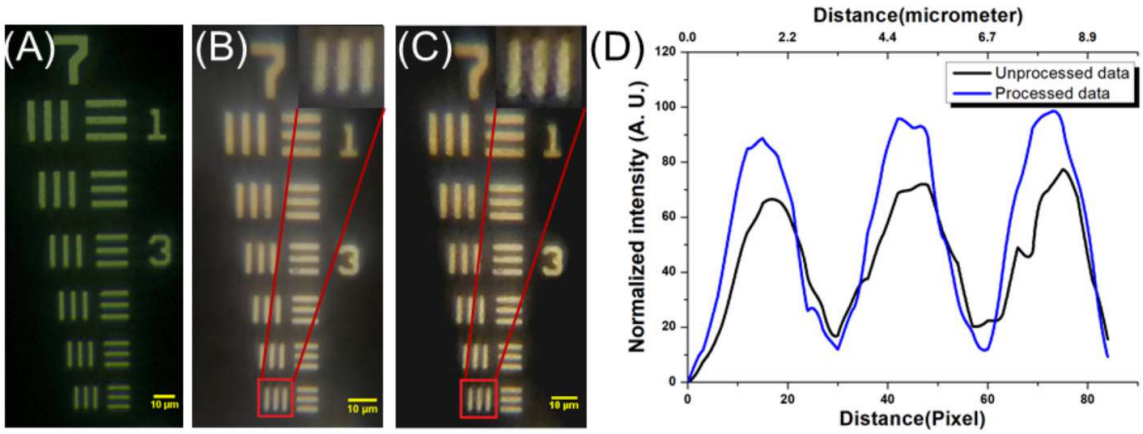

Figure 4.7: Images of USAF Resolution test target (A) obtained from standard optical microscope (Carl Zeiss's Primo Star), (B) with the designed smartphone based optical microscope, (C) its corresponding processed image and (D) intensity profile of the selected region. Scale bars are 10 μm.

image. After several cycles of evaluations, an optimum value of 'disk' type PSF with estimated noise-to-signal ratio (NSR) of additive noise has been used to deconvolve the image. To remove the ringing effect and peculiar blur on the edges due to deconvolution operation, an *'edgetaper'* function has been implemented before calling the *'deconvwnr'* function from the library. A 2×2 median filter is then used to smooth and remove the noise present in the deblurred image. Developing an image processing applications in the cloud offers two important advantages-(i) the processed image from the cloud can be obtained almost instantly upon uploading the captured image in the server, and (ii) with a moderate processing speed of all regular smartphones, the performance of the phone processor may degrade if the image processing application is run within the phone itself. This would take a relatively long period (up to several minutes) to obtain the processed image from the raw data. This can be avoided if the application is developed in the cloud. Moreover, a regular smartphone may not have sufficient storage capacity for storing the captured images within the phone. Using cloud-based facilities the captured images can be stored externally. Matlab mobile from MathWorks is available free of cost for both android and iOS platform smartphones. With the wide availability of smartphones and ever-increasing coverage of mobile broadband network namely the Global System for Mobile (GSM) and Long Term Evaluation (LTE) networks, a new possibility of accessing cloud-based services has emerged in the recent years.

4.2.3 Optical characterization of the tool

Magnification and resolution

Prior to evaluating the performance of the proposed smartphone microscope, its optical magnification has been estimated. The optical magnification of the designed microscopic system can be estimated as

$$M_{total} = M_1 \times M_2 \tag{4.1}$$

where $M_1 = \frac{1000(n-1)}{nD}$ is the magnification obtained from the ball lens, n is the refractive index, D is the diameter of the ball lens, and $M_2 = 1+\frac{d}{f}$ is the magnification due to the PCX lens used. With 1 mm diameter ball lens (RI = 1.517) and 6 mm diameter (d) PCX lens (focal length, f = 11 mm), the net optical magnification of the designed microscopic system is thus estimated to be ∼520× [11].

The resolution of the designed tool has been estimated through imaging of 1951 USAF resolution test target. The resolution of the designed tool is calculated using the following equation:

$$Resolution(\frac{lp}{mm}) = 2^{Group\ number + \frac{Element\ number-1}{6}} \tag{4.2}$$

here, the group and element number refer to the clearly resolvable white and black bars on the target element captured by the designed system. By taking the reciprocal of the lp/mm (line pairs per millimeter) and multiplying it by 1000, the resolution of the designed microscopic system can be converted to micrometer (μm) scale. Figure 4.7(A) shows the image of the target element captured by standard optical microscope (Carl Zeiss's Primo star, Germany) while figure 4.7(B) shows the image of the same element captured by our designed smartphone microscope. Element 6 of group 7, which is the highest resolved line element of the target can be imaged clearly by the proposed microscopic system. The resolution of the designed optical tool is estimated to be ∼2 μm which is slightly lower than the theoretical resolution ($R_{th} = \frac{0.61\lambda(=550nm)}{NA(=0.249)} = 1.34\mu m$) for a 1 mm ball lens while using it as an objective lens. In order to enhance the imaging quality of the captured images, the cloud-based application has been implemented for post-processing and subsequently access the processed image from the cloud server. Figure 4.7(C) illustrates the processed image of the considered region of the target element which has been obtained upon processing it from the cloud. The enhancement in the resolution quality of the processed image has been compared with its unprocessed image. Figure 4.7(D) illustrates the intensity profiles of the selected regions (indicated in red square in figure 4.7(B) and (C)) of the target element. Clearly, the figure shows that with the aid

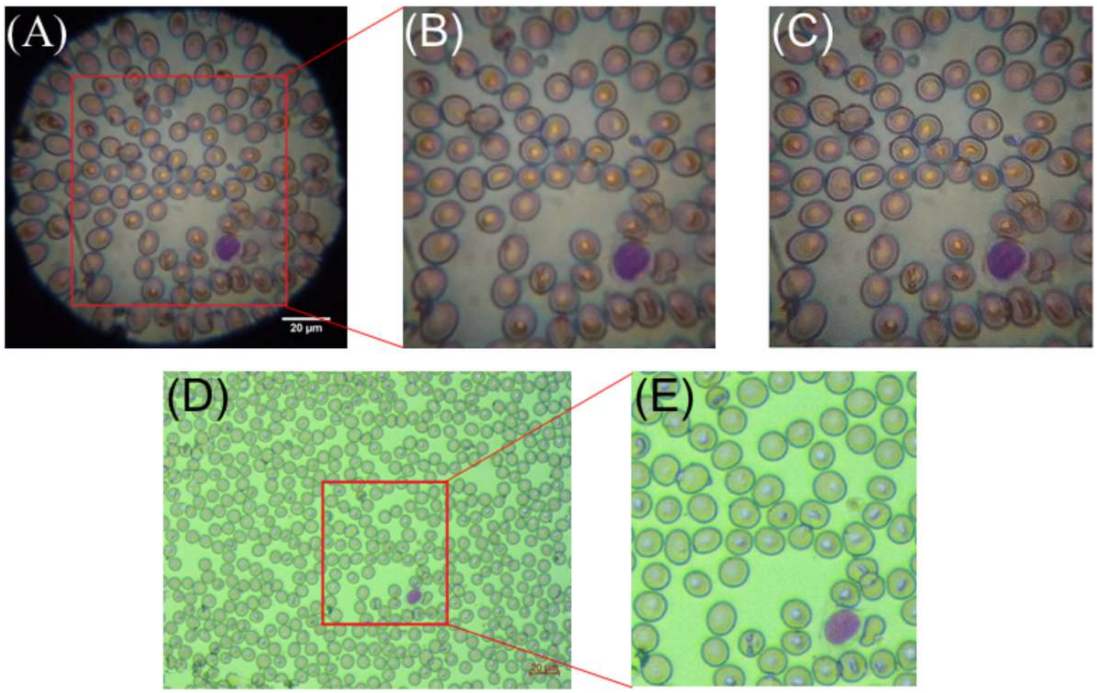

Figure 4.8: Processed smartphone microscope image of thin blood smear. (A) Smartphone microscope image, (B) corresponding image of a cropped region, (C) corresponding processed image of the cropped region (D) a 40×/0.65 NA traditional microscope image of the blood sample and (E) zoomed version of the same region of interest (ROI) of the traditional microscope. Scale bars are 20 μm.

from the cloud, the resolution quality and the signal-to-noise ratio of the captured images have been improved significantly upon processing it in the cloud.

4.2.4 Imaging of biological specimen and comparison of the results with standard tool

The field applicability of the proposed microscopic tool has been evaluated through imaging of red blood cells (RBCs). Leishman stained blood sample has been acquired from the pathology laboratory of Tezpur University health centre. Figure 4.8(A) shows the image of the RBCs captured by the designed smartphone microscope while figure 4.8(B) represents the cropped region of the captured image indicated in red square in figure 4.8(A). Upon processing the cropped region in the cloud, significant improvement in the image in terms of sharpness and resolution has been noticed. The resultant processed image is shown in figure 4.8(C). For reference, the figure also includes the photo image of the same blood smear captured by the standard optical microscope (Carl Zeiss's Primo Star) using a 40×/0.65 NA objective lens. Figure 4.8(D) represents the image of the same region of the blood sample shown in figure 4.8(A) captured by the optical microscope. Figure 4.8(E) shows the cropped area as indicated in red square in figure 4.8(D). Clearly, from the figures 4.8(C) and (E), it

can be inferred that the quality of the post-processed image is same as that of the standard optical microscope in terms of resolution and sharpness. This suggests that the designed microscopic tool can be reliably used for imaging of any micron-scale particles.

Quantitative analysis of the captured images by the smartphone microscope in terms of structural similarity index (SSIM) and the peak signal-to-noise ratio (PSNR) with reference to the laboratory-grade microscope has been studied using the following equations [12, 13]:

$$SSIM(x,y) = \frac{(2\mu_x\mu_y + C_1)(2\sigma_{xy} + C_2)}{(\mu_x^2 + \mu_y^2 + C_1)(\sigma_x^2 + \sigma_y^2 + C_2)} \tag{4.3}$$

where, μ_x, μ_y, σ_x, σ_y, and σ_{xy} are the local means, standard deviations and cross-covariance for the images x and y. C_1 and C_2 are dummy variables.

$$PSNR = 10\log_{10}\frac{peakval^2}{MSE} \tag{4.4}$$

where, *peakval* is the maximum signal value that exists in the original image and MSE is the mean squared error between the two images. The SSIM value is found to be 0.5702 while the PSNR value is estimated to be 14.5192 dB. The moderate level of SSIM and PSNR are attributed to the variation of the optical components involved in both the systems. The optics design and the features of the CMOS imaging sensors for both the tools are not identical due to which imaging qualities are found to be varied. However, while estimating the SSIM and PSNR value for the same captured images by the designed smartphone microscope, a significant improvement of these parameters has been noticed. For a processed image with reference to its original image captured by the designed smartphone microscope, the SSIM and PSNR values were measured to be 0.8740 and 34.028 dB, respectively.

4.2.5 Discussion

The 3D printed optical setup which holds the ball lens also serves as an aperture (diameter 0.7 mm) for the proposed optical system. This helps to eliminate the peripheral rays and subsequently improves the overall imaging quality by minimizing the spherical aberration that may present in the designed microscopic system. The optical FoV of the designed smartphone microscope is estimated to be ~150 μm (diameter). With the incorporation of 3D printed XY stage which has been used for holding the sample, it is possible to image over an area of 10 mm × 10 mm. Table 4.1 summarizes the figure of merits of the designed microscope in terms of its magnification, resolution, FoV, cost involvement, portability and data-sharing ability

Table 4.1: Comparison of the figure of merits between a standard optical microscope and the designed smartphone microscope.

Parameters	**Optical microscope**	**Smartphone microscope**	**Remarks**
Magnification	400× (using 40×/0.65 NA objective lens)	∼520×	With 520× optical magnification, it is possible to image any sub-micron scale particles.
Resolution	∼0.42 μm	<2 μm (based on USAF target element)	Using custom-designed application, the resolution of the designed microscope can be enhanced further.
FoV	∼334 μm (diagonal)	∼150 μm (diameter)	Lower FoV has been noticed due to the introduction of the aperture in the setup.
Cost	∼USD 3000.00	<USD 250.00 (including the smartphone)	The net cost involved is ten times less than its commercial counterparts.
Portability	No	Yes	Owing to its compact size, the designed microscopic system can be used for in-field applications.
Data-sharing ability	Yes (requires dedicated internet connectivity through Wi-Fi or Ethernet cable)	Yes	Using the mobile broadband network, the field-collected data can be shared anywhere in the world instantly.

and compares these parameters with respect to a standard optical microscope.

It is essential to mention the challenges and drawbacks that may arise due to the miniaturisation of the designed smartphone optical microscope. The use of ball lens as an objective lens causes a spherical aberration as well as distortions at the peripheral region of the captured image. The ball lens holder is designed in such a way that only the focused region of the image enters the smartphone camera and the peripheral-rays contributing to the spherical aberrations is eliminated from entering the ball lens. Since it provides high magnification without much complication, ball

lenses are of natural choice for the development of high magnification optical tools. 1 mm ball lens provides an optical magnification of ∼340× and the plano-convex lens with a focal length of 11 mm and a diameter of 6 mm contributes a magnification of ∼1.54×. The combination of these two lenses yields an overall optical magnification of ∼520× in the present optical system.

4.3 Optimization of the smartphone microscopic system for fluorescence imaging and onsite cell counting applications

BF and fluorescence microscopes are the most indispensable and widely used microscopic techniques for biological research, environmental monitoring, biomedical study, clinical diagnostics and other areas [14, 15]. In the BF mode of imaging, the resulting image is primarily absorption-based, while specimens lacking intrinsic absorption cannot be visualized with a good degree of contrast. For such cases, the fluorescence mode of imaging is useful, which can be obtained through encoding the specimen using endogenous or exogenous staining. This mode of imaging allows highly sensitive and precise detection and tracking of cells, proteins, and other molecules of interest in the specimen [16]. A conventional microscope with BF and fluorescence imaging features is typically built by integrating several modules, including high-performance optics such as filters, objective lens, imaging sensors, a mechanical part for holding and a dedicated computer for image recording and analysis. Eventually, this has made the conventional imaging system costly (>USD 6000.00), heavy, fragile, and requires routine maintenance, thus restricting the use of the conventional microscopic system at the PoC level and also in resource-constrained settings [17]. It is, therefore, important to develop a portable, cost-effective microscopic system with BF and fluorescence imaging features that could facilitate its deployment in resource-poor settings.

In this section, the $4f$ optical configuration described in the section 4.2 has been further extended to develop an affordable, miniaturized BF and fluorescence microscopic system on a smartphone platform. The designed imaging system has a varying optical magnification (from low to high) and has an optical resolution of approximately 1.21 μm. The $4f$ optical imaging configuration has been further optimized in the proposed microscopic system by using off-the-shelf optical and easily available electronic components. A 3D-printed optical setup houses the designed configuration which can be integrated to the rear camera of the phone. The pre-built camera application of the phone has been utilized for image acquisition and storing in the phone. The proposed technique has an ability to transform any smartphone into a

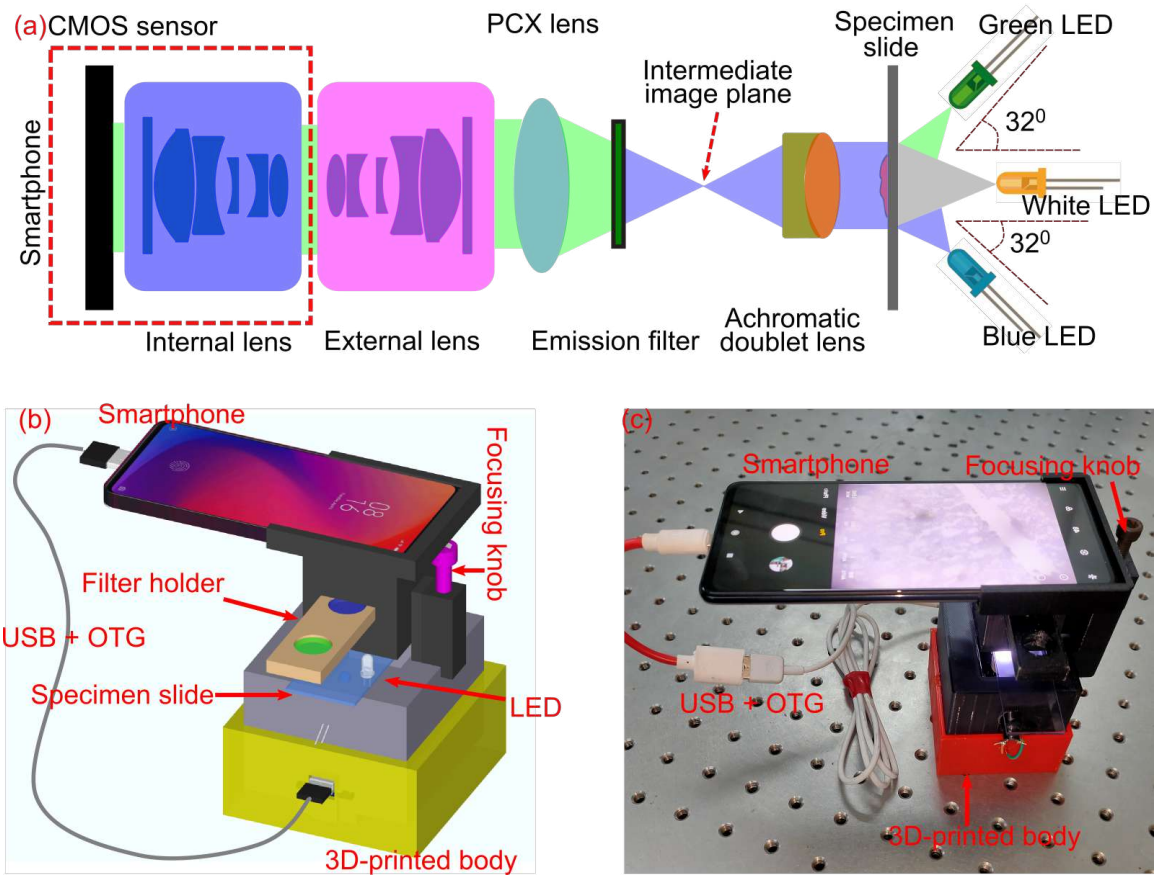

Figure 4.9: Design of the proposed BF and fluorescence microscopic device. (a) Optical layout diagram of the system; (b) 3D design of the system; (c) Fully assembled device in working condition.

standalone, portable, inexpensive multimodal microscopic system. The applicability of the designed platform is demonstrated by imaging standard microbeads and biological specimens and compared the results acquired from the standard microscopic system. Besides, with another custom-designed application, the designed imaging platform has been used to study cell recognition and count from the captured images of blood samples. The following subsections discuss the detailed design and operation of the proposed imaging system along with its performance.

4.3.1 Working Principle

Design of the bright-field and fluorescence imaging system using a smartphone

Figure 4.9(a) depicts the schematic of the proposed microscopic system. The imaging system has been designed in such a way that recording of the images from the specimen can be performed with minimal aberrations and distortions throughout the FoV. For the fluorescence mode of imaging, the emitted light from the specimen is

collimated by using an achromatic doublet lens, and the emitted fluorescence signal is allowed to pass through a band-pass filter to eliminate the excitation wavelength from reaching the imaging sensor of the phone. Another plano-convex lens focuses the collimated light signal and is coupled to the CMOS sensor of the phone. Smartphone cameras, in general, are not designed for microscopic imaging, thus need additional optical elements to reduce aberrations and distortions due to the high angle collection and multiple wavelengths of light from the specimen. The simplest and cost-effective way to resolve this issue is to use another smartphone camera lens in reverse orientation [18, 19]. This lens is a perfect alternative for the proposed motive because of its low-cost and high NA with an overall good optical performance and minimal aberrations over a wide FoV (several mm). For this specific configuration, the designed imaging system performs at its highest potential by fully utilizing the maximum NA of the objective lens. BF imaging can be obtained in the same setup simply by removing the emission filter from the optical path.

The major components of the proposed setup comprise of imaging optics, illumination optoelectronics, a z-translational stage for focusing and a plastic housing to hold all the components. The 3D layout and photo image of the proposed microscopic system are shown in figures 4.9(b) and (c), respectively. It consists of Redmi K20 smartphone from Xiaomi Inc. This phone is equipped with a primary Sony IMX582 CMOS camera sensor of 48 MP that has a pixel dimension of 0.8 μm along with an inbuilt lens of f-number 1.75 (FL = 4.77 mm, NA = 0.28). By default, it records images with a pixel dimension of 1.6 μm (four pixels of 0.8 μm combined to form a single large pixel of 1.6 μm). The miniaturized microscopic attachment as constructed and depicted in figure 4.9(a) includes an achromatic doublet lens (D = 4 mm, FL = 6 mm, NA = 0.33, #63-714, Edmund Optics) or a ball lens (D = 3 mm, #43-711, Edmund Optics) as an objective lens, a plano-convex lens (D = 6 mm, FL = 11 mm, Holmarc Opto-mechatronics Pvt. Ltd.) as a tube lens, iPhone 5s rear camera lens (FL = 4.12 mm, NA = 0.23, $f/2.2$, Amazon.in) as a relay lens, and bandpass optical filter (center wavelength, CWL = 520 nm, #67-016, Edmund Optics) for imaging in fluorescent mode. The overall optical magnification, resolution and the FoV of the designed optical system vary with the type of lens being used as an objective lens in the setup. For instance, with an achromatic lens as an objective lens, one can achieve a relatively low magnification and limited FoV. However, the imaging system receives fluorescence signals with a high SNR from the specimen. Again, for high magnification, a ball lens (3 mm) can be used, but it yields a limited FoV in the imaging plane of the microscopic system. With the iPhone reverse camera lens as an objective, the proposed platform yields the lowest optical magnification but provides a large FoV with minimal aberrations. In the illumination panel, a white LED has been used for BF imaging, while another two LEDs that emit blue and green light

with peak emission wavelengths 490 nm and 525 nm respectively have been used for fluorescence-based imaging purposes. The blue and the green LEDs have been kept at an oblique angle of 32° so that the excitation light from the source couldn't enter the objective lens directly. This arrangement would enhance the SNR in the final fluorescence image, and the use of excitation optical filter into the system can be obviated. The LEDs have been powered from the smartphone battery using the open-access android application *'Serial USB Terminal'*. The illumination from these LEDs can be controlled from the phone through a microcontroller board (NodeMCU ESP32, Amazon.in) as an interface. Serial communication has been established between the android application and the microcontroller, which would control the illumination for the proposed microscopic system.

4.3.2 Materials and methods

Fabrication and alignment of the microscopic system

Precise optical position and alignment are critical for any microscopic imaging setup. In the present study, a distance of 35 mm has been maintained between the objective lens and the PCX lens. An external camera lens has been placed between the PCX and camera lens of the phone to optimally couple the final image to the CMOS sensor for image recording. An emission filter is positioned between the PCX and the objective lens for the fluorescence mode of imaging. The microscopic module has been designed using ZW3D software and fabricated in a 3D-printer (Raise N2) with polylactic acid (PLA) as a printing material. All the optical components have been mounted on this 3D-printed cradle and coupled it to the rear camera of the phone. Besides, the designed optical system also has a 3D-printed z-stage which has been used for focusing the specimen. There are six 3D-printed blocks that houses different optical components, and assembled into a single block to attach it to the phone. The overall dimension of the system 11.5 cm × 7.5 cm × 6.5 cm and its net weight, including the phone, is ∼341 gm.

Image acquisition and analysis

The inbuilt camera application of the phone has been utilized to record the images of the microscopic system. It is the primary choice since it can provide advanced control over the imaging parameters such as ISO (gain), exposure time, focus and white balance. The phone camera application generally processes raw image data recorded by the CMOS sensor using its internal data processing algorithm and saves it in 24-bit RGB color images (JPEG compression). However, one can access the raw data of the sensor by using third-party applications such as Open Camera by

Mark Harman. This is useful for precise quantitative analysis of the sample where acquisition of raw data plays an important role. For the present imaging system, the ISO has been maintained in the range of 200-400 to obtain an optimum SNR, and the exposure time has been maintained between 125 milliseconds to 2 seconds, depending on the specimen types and dye concentration. Image parameters analysis such as FoV measurement, cell size measurement, and adding of scale bars in the images can be done using ImageJ (Fiji) software. For cell intensity variance measurement and testing the cell recognition algorithm, Matlab platform (version 2017b) has been utilized.

Sample preparation

Fluorescent microbeads of 1 μm diameter (Sigma Aldrich, $\lambda_{ex} = 490$ nm, $\lambda_{em} = 525$ nm) have been diluted in distilled water and dispersed on a microscopic slide for imaging. Blood samples from 10 different patients have been collected in EDTA-treated tubes from Tezpur University Health Centre. For BF imaging, blood samples were initially stained using Leishman solution. For fluorescent imaging, blood cells were stained with acridine orange with a concentration of 0.047 mg/mL. Acridine orange will stain only the WBCs leaving the RBCs unstained. For cell counting, the RBC and WBC blood cells are diluted in Hayem's and Türk's solution (Sigma Aldrich), respectively. Hayem's solution can be synthesized in the laboratory by treating 0.25 g Mercuric chloride ($HgCl_2$), 0.5 g sodium chloride ($NaCl$), 2.5 g sodium sulphate (Na_2SO_4) in 100 ml distilled water.

4.3.3 Optical characterization

Determination of magnification, resolution, PSF and FoV

For the present imaging system, the total optical magnification depends on the configuration of the optics and can be represented as $M_t = \frac{f_s}{f_o} M_r$, where f_s is the focal length of the smartphone camera lens, f_o focal length of the objective lens and M_r magnification of the relay or coupling lens [19]. For the different objective lenses as considered in the present study, M_t is found to be 1.16×, 2.86× and 37.33× corresponding to the reverse camera lens of iPhone 5s, achromatic doublet lens and 3 mm ball lens, respectively, while using it as an objective lens in the setup. For the smartphone with a screen size of 6.39 inches (diagonally) with an aspect ratio of 19.5:9, and with an imaging sensor dimension 8 mm (diagonal), the displayed image will have an extra digital magnification of ($M_d = \frac{Size_{screen}}{Size_{sensor}}$) $M_d = 20.3\times$ on the phone's screen.

In its bright-field mode, the lateral resolution of the microscopic system has been estimated by imaging a standard 1951 USAF resolution test target. Figure 4.10(a)

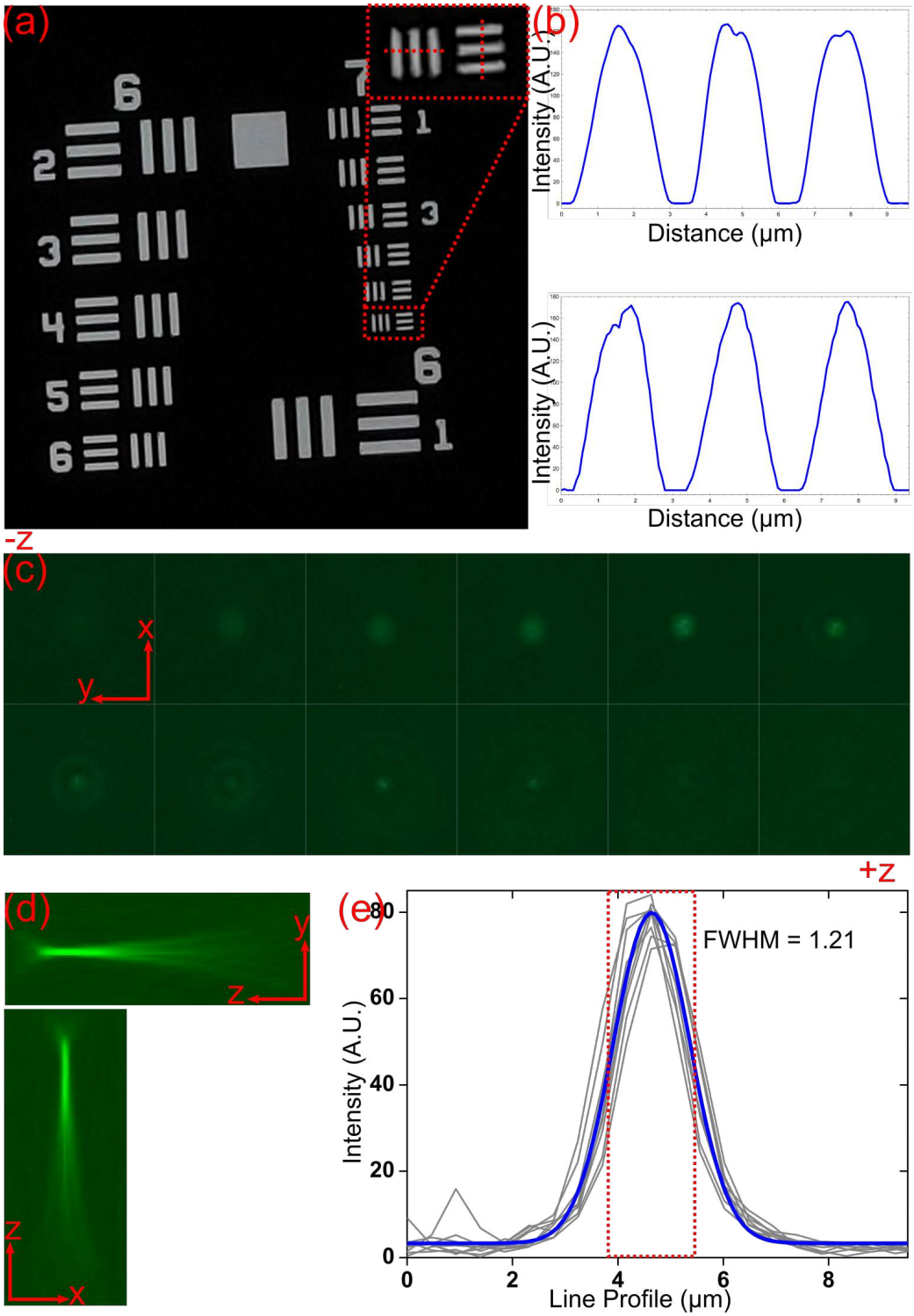

Figure 4.10: Characterization and performance testing of the microscopic device. (a) Image of a USAF-1951 resolution test target acquired under BF illumination showing spatial resolution of the microscopic system up to Group 7 Element 6 (2.19 μm); (b) Represents the intensity profile of the horizontal and vertical element bars of Group 7 indicated in dotted red line in fig. (a); (c) 12 images of the PSF in x-y direction of 1 μm microbeads focused from –z direction to +z direction; (d) Reconstructed PSF from (c) in y-z and x-z direction; (e) Measurement of the FWHM of the PSF in lateral direction by taking average values of 10 microbeads within a single FoV.

illustrates the images captured by the proposed tool. A group of bars, both in horizontal and vertical orientation are defined to be resolved if the contrast ($C = \frac{I_{max}-I_{min}}{I_{max}+I_{min}}$, I_{max} is the maximum intensity of the bars and I_{min} is the minimum intensity of the bars) exceeds by 10%. The objective lens of the present microscopic system has a NA = 0.33. Thus, the theoretical diffraction-limited resolution for the designed platform would be 1.02 μm ($r_{diff} = \frac{0.61\lambda}{NA}$, $\lambda = 550$ nm). Experimentally, under white light illumination, the resolution is measured to be 2.19 μm, and it can resolve the highest group element bars that are the group 7 element 6 of the resolution target, as shown in figure 4.10(b).

To estimate the resolution of the designed platform, 1 μm diameter fluorophore beads have dispersed on a microscopic slide and excited with a 490 nm wavelength. The corresponding fluorescent signal from the microbeads has been captured by the phone camera after allowing it to pass through a 520 nm bandpass emission filter. Figures 4.10(c) and (d) show the PSF of one such microbead in x-y, y-z and x-z directions. Figure 4.10(c) shows 12 images of the 1 μm bead, which have been acquired sequentially while focusing from –z direction to +z direction. It is evident that the airy disk patterns appear only in one direction when the focusing goes in the +z direction. On the other hand, the image becomes blur when the focusing knob moves in the reverse direction without forming any airy pattern. Due to this, there is an asymmetry in the PSF that can be clearly seen from the orthogonal views, as shown in figure 4.10(d), indicating the presence of spherical aberration in the designed system. Figure 4.10(e) illustrates the line profiles of the 10 different microbeads. For a given spatial position, the resolution can be defined as the full width at half maximum (FWHM) of a normalized Gaussian-fitted curve on the experimental data points of the PSF. The thick blue line in figure 4.10(e) represents the Gaussian-fitted curve of average line profiles of the imaged microbeads. The lateral resolution of the system is found to be ~1.21 μm as compared to the theoretical value of 1.02 μm stated above. The FoV of the system is measured to be ~4530 μm, 400 μm and 200 μm in diameter while using the iPhone camera lens and achromatic doublet lens and ball lens as an objective, respectively.

4.3.4 Practical applications of the microscopic system

BF and fluorescence imaging of blood cells

Assessing the ability of the developed microscopic system to perform high-quality imaging of biological specimens is of particular interest. Examining blood samples under a microscope is the first necessary step for screening various diseases. A reliable imaging of blood cells has been prioritized to test the validity and the performance of the designed microscopic system. Figure 4.11(a) shows the BF image of the captured

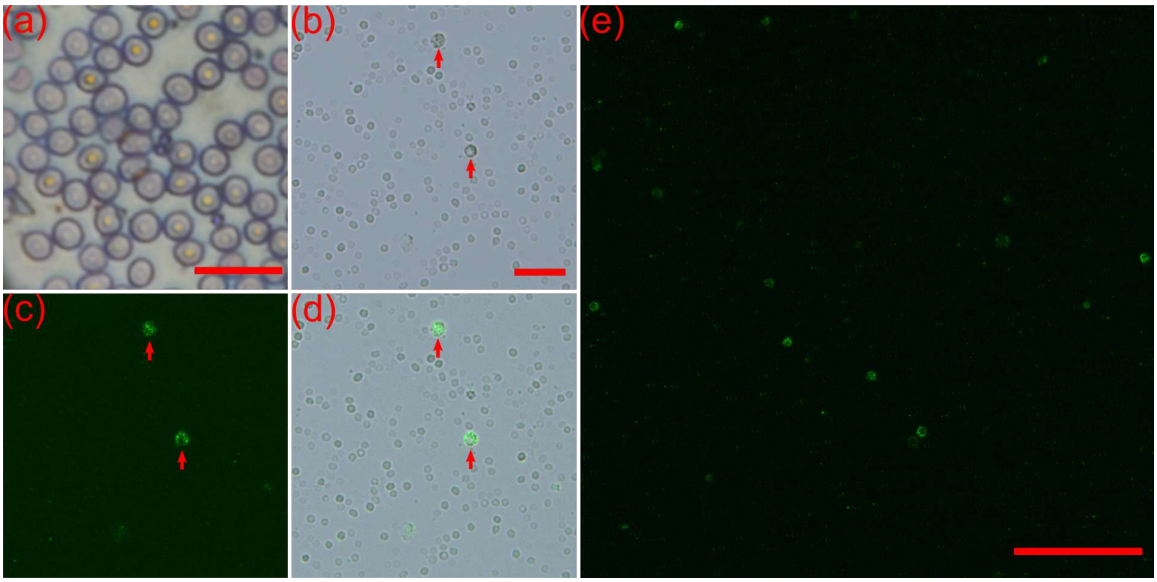

Figure 4.11: Applications of the microscopic device for imaging of biological specimen. (a) Leishman stained blood smear image captured using the proposed device under BF illumination. Scale bar is 20 μm; (b) BF image of the Acridine orange stained blood; (c) Fluorescence image of the same region in (a); (d) Overlaid image of the BF and fluorescence image of blood shown in fig.(b) and (c). Scale bars are 50 μm; and (e) a large FoV of the fluorescence image of whole blood. Scale bar is 200 μm.

blood smear by our designed microscopic system. Fluorescence imaging of whole blood samples is often used to characterize WBCs for different applications, such as distinguishing and counting different types of leukocytes present in the samples. To illustrate the high-throughput performance of the system, fluorescence imaging of WBCs in the whole blood sample has been performed. The acridine orange-stained blood specimen has been excited by a 495 nm LED source. The fluorescence emission from the specimen at 520 nm has been captured by the camera of the phone. The recorded images under BF and fluorescence modes are shown in figures 4.11(b) and (c), respectively. Figure 4.11(d) represents the overlaid image of figures 4.11(b) and (c). Figure 4.11(e) shows a large FoV of the fluorescence image of the whole blood sample. It is apparent that some of the WBCs in the FoV are out of focus in the imaging plane attributed to the limitation of the 3D-printed manufacturing of the device's specimen holder. Acridine orange binds strongly to double-stranded DNA. In this case, the excitation and emission wavelengths are 502 nm and 525 nm, respectively. Besides, the same staining dye also binds strongly to single-stranded DNA and RNA. For this case, the excitation and emission wavelengths are found to be 460 nm and 650 nm, respectively. Thus, blood samples stained with acridine orange emits fluorescence signal both in green and red upon excitation with the respective wavelengths. However, the emission of cell cytoplasm is predominantly in the red region because of the presence of RNA and lysosomes. This phenomenon

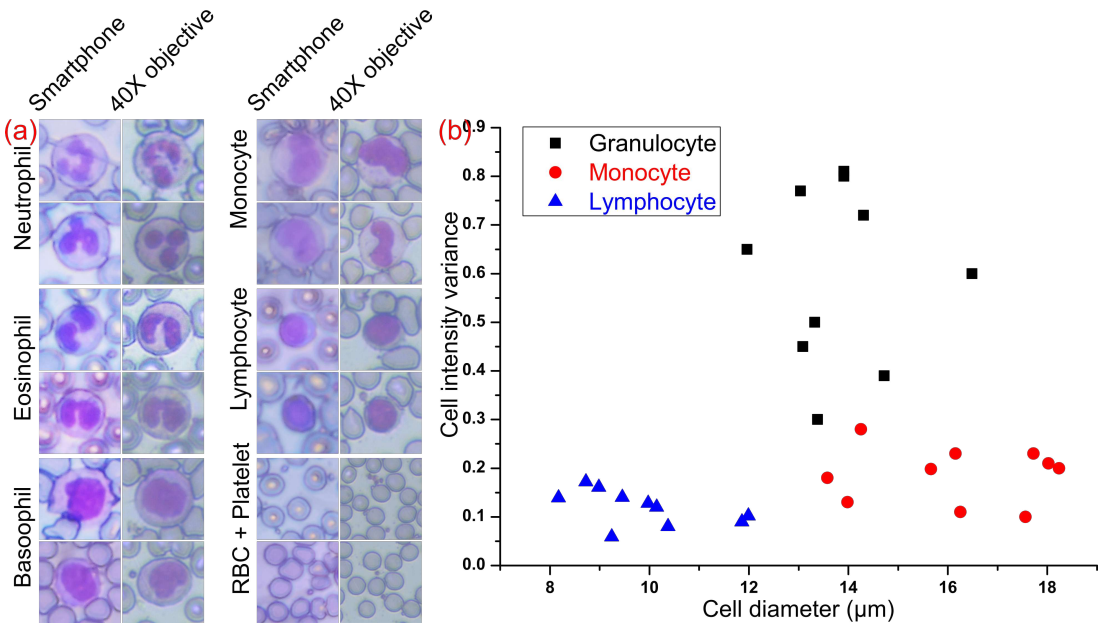

Figure 4.12: Application of the microscopic device for morphological study. (a) Comparison of images of five types of WBCs (Neutrophil, Eosinophil, Basophil, Monocyte, and Lymphocyte), RBCs and platelets acquired using the proposed microscopic system and a laboratory-grade microscope, respectively. (b) Scatter plot of the cellular intensity variance against cell diameter to perform a three-part WBC differential where black color represents the granulocytes, red for monocytes, and blue for lymphocytes.

can be used for sorting WBCs by estimating signal intensities in red-to-green ratios [20]. By simply replacing a bandpass filter with a 520 nm long-pass filter, this can be easily performed with the designed microscopic system.

In some applications, manual microscopic examination is required to confirm and evaluate the morphology of blood cells [21]. Figure 4.12(a) illustrates the comparison of the BF images of RBCs, five different types of WBCs and platelets captured using our microscopic setup and a traditional laboratory microscope (Carl Zeiss's Primo Star). The figures clearly indicate that the designed imaging platform can reliably produce and recapitulate morphological features of blood cell phenotyping and differentiation. Again, three different classes of WBCs-granulocytes, lymphocytes and monocytes have been distinctly imaged by the proposed platform and can be distinguished easily based on the granularity and size of the cells. Figure 4.12(b) represents the scattered plot of the cell diameter against the intensity variance throughout the cell. The plot clearly shows the class separation between these three different WBCs that exhibit different ranges of intensity variance, which can be sorted based on their granularity. For instance, the granulocyte produces the highest intensity variance due to its higher granularity compared to monocyte and lymphocytes.

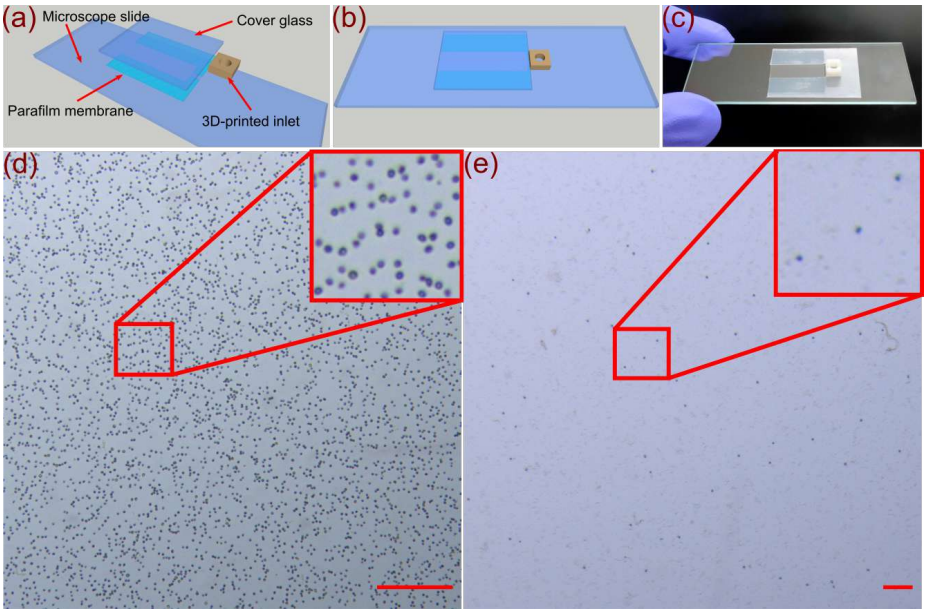

Figure 4.13: Application of the microscopic system for cell concentration counting. (a) 3D layout design of the DIY chamber; (b) Assembled chamber; (c) Fabricated sample loading chamber chip; (d) BF image of diluted RBCs captured under low magnification of the proposed microscopic system. Inset image shows the zoom-in view of the ROI marked in red square. Scale bar is 100 μm; (e) BF image of diluted WBCs. Inset image shows the zoom-in view of the ROI marked in red square. Scale bar is 200 μm.

Application of the microscopic system for cell counting

Finally, onboard automatic cell counting has been performed to demonstrate the versatility and applicability of the developed microscopic system. Cell counting is routinely performed in many applications, especially in clinical laboratories for disease diagnostics and biological detections [6, 22, 23]. To demonstrate the ability of the present system to perform these features, total RBCs and WBCs have been counted with the designed system and compared the results with a widely used traditional manual counting technique using a hemocytometer. To make the sample loading process relatively simpler, a DIY chamber has been fabricated using the commonly used microscopic slide, a parafilm membrane, a cover glass and a 3D-printed inlet. As shown in the figures 4.13(a)-(c), the DIY chamber has been fabricated by making a channel from the cut out of a parafilm and placed on a microscopic slide. The top of the film is covered with a cover glass, and a 3D-printed inlet is coupled to it through heat-fixed. The channel depth of the DIY chamber is found to be ~0.1 mm. Upon loading the sample into the inlet, it spreads uniformly throughout the channel by the capillary action. For total WBC counting, 20 μL of blood has been mixed with 400 μL of Türk's solution to obtain a dilution factor of 1:20. This specific solution would lyse the RBCs so that only the WBCs will be visible under the microscopic setup. Thus, the number of total WBCs can be easily counted. Similarly, for RBC counting,

the whole blood is mixed with freshly prepared Hayem's solution at a dilution factor of 1:200. Hayem's solution lyses the WBCs to distinctly capture the images of RBCs by the microscopic system. 10 μL of each diluted sample have been loaded on the hemocytometer and the laboratory-designed DIY chamber, and allows to settle the cells before imaging with our designed system. The manual counting on the hemocytometer has been performed on a laboratory microscope at low magnification. The image acquisition for automatic cell counting has been performed using the developed microscopic device at low magnification as shown in figures 4.13(d) and (e) and a custom-designed android application.

A cell recognition algorithm has been developed for cell counting by importing the OpenCV library to the android platform. Figure 4.14 illustrates the flowchart of the algorithm. First, the classical Sobel operator has been implemented to recognize the edges of the cells. This operator convolved with the BF image in figure 4.14(a) by using two 3×3 kernels. After that, it is converted to a binary image by applying the thresholding operation shown in figure 4.14(c). To remove the unwanted artifacts and noise in the threshold image, erosion and dilation operation have been implemented. Figure 4.14(d) represents the captured images of the cells after performing the above-mentioned steps. Now, by applying the contour detection technique shown in figure 4.14(e), the total number of cells present in the FoV can be calculated automatically. The android application has been developed based on this algorithm, and the user interface is shown in figures 4.14(f), (g) and (h).

The custom-developed cell counter app has been deployed for counting the RBCs and WBCs in the whole blood sample. The counting results are compared with the traditional manual counting using a hemocytometer. It is found that for dilution at 1:20 for WBC and 1:200 for RBC, the designed imaging platform can quantify all the cells in its FoV. Figures 4.15(a) and (b) illustrate the comparison of RBC and WBC counts that have been performed through manual counting and by the designed smartphone automatic counter. The blood counts of 10 different samples collected from different human subjects have been performed. A normal blood count has RBCs and WBCs in the range of 4-7 $\times$ 106 /μL and 4-10 $\times$ 103 /μL, respectively. Our automated counting system yields results that lie within these ranges. A good degree of correlation is observed between the manual count and the smartphone-based automated counter. For RBC counting, the correlation coefficient is found to be $R^2 = 0.94657$, while for WBC, this value is found to be $R^2 = 0.94596$. These data signify a high degree of reliability of the proposed technique while using it for cell counting applications.

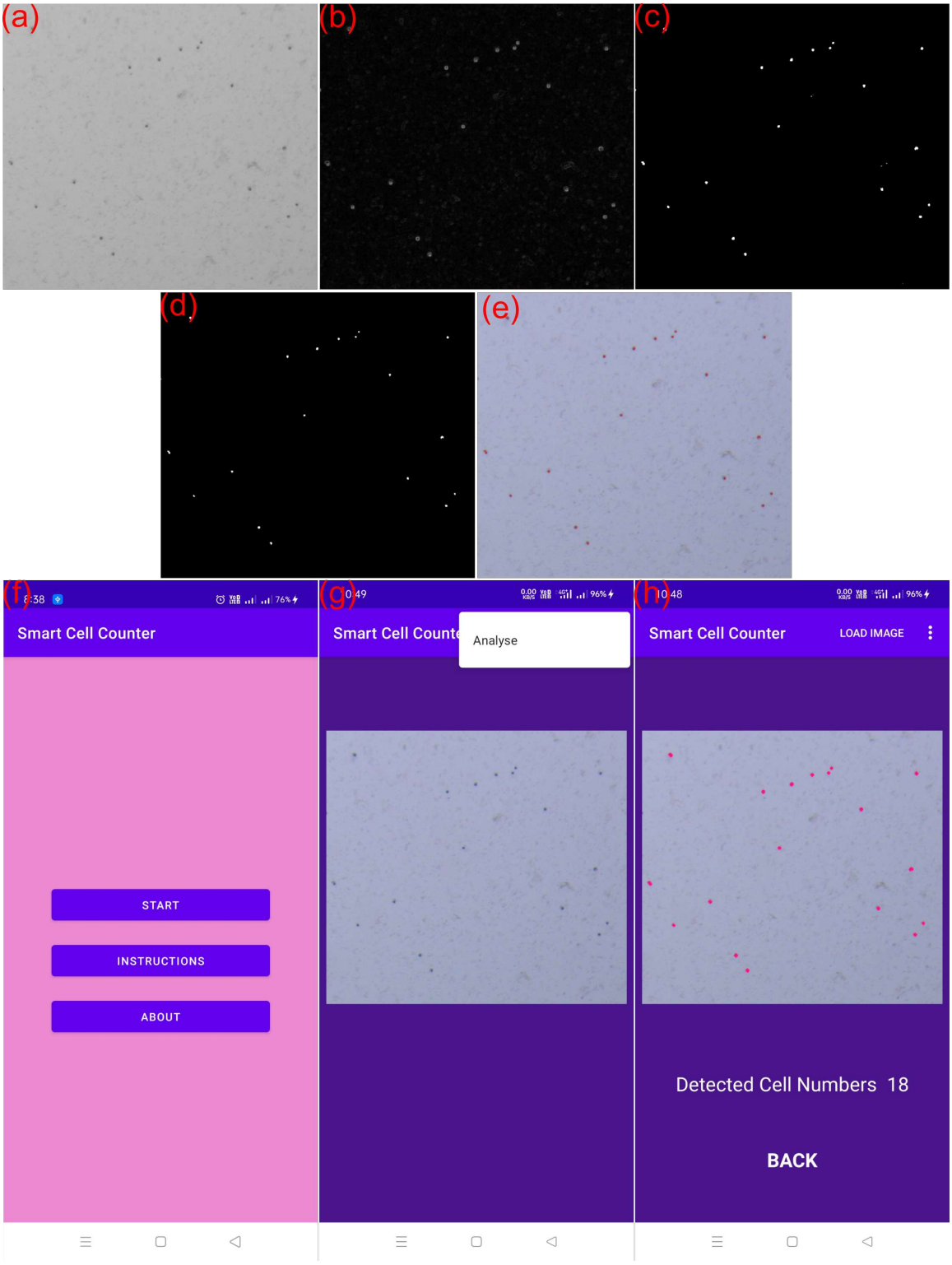

Figure 4.14: Development of the cell recognition and counting algorithm and the interface of the android application. (a) BF image of cells in a single FoV; (b) Implementation of the Sobel operator to recognize the cell boundaries; (c) Thresholded image; (d) Recognized cells after the removal of noisy artifacts; (e) Cell number estimation using contour detection algorithm; (f) initial interface of the android app; (g) BF image read-in; (h) Output results.

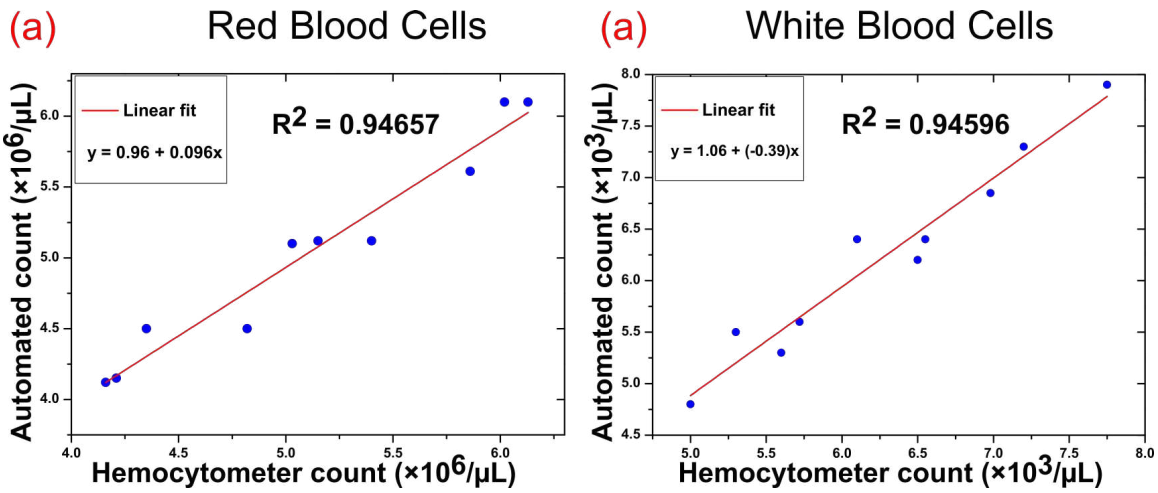

Figure 4.15: Comparison of our developed automatic microscopic system counting results with the manual hemocytometer count that traditionally used in clinics. (a) Results for red blood cells counting where red line represents the line of perfect prediction for both the cases. (b) Counting results for white blood cells. A consistent count of both RBCs and WBCs are observed.

4.3.5 Discussion

Many improvements of the microscopic design over the previous platform have been done in this section of the chapter. The optical design has been optimized for high-quality imaging over the entire FoV with minimal aberrations and distortions at a very low cost, which is comparable to laboratory-grade systems. The proposed system utilizes the full potential of the objective lens, providing a diffraction-limited resolution by employing the $4f$ configuration of an imaging system. One of the major setbacks of the previously reported smartphone microscopes was the fixed magnification of the system. Herein, three different optical magnifications have been demonstrated in this work, which can also be increased further as per the requirements. This is suitable and indispensable for different biological applications. Even though yet there are immense scopes of further optimization of the developed prototype.

The above experimental findings suggest that the designed system has the ability to image and assess both the morphology of individual cells and the cell population statistics. The proposed platform can be reliably used in clinical laboratories, and has been developed as a proof of concept, which could be further optimized in terms of its costs and performance. The net material costs involved to develop the proposed imaging platform, excluding the smartphone, is approximately USD 448.8 only, and detailed breakup is shown in the table 4.2.

Table 4.2: List of essential components for the construction of the proposed smartphone microscopic system.

Sl. No.	**Component**	**Quantity**	**Source/Supplier**	**Cost ($)**	**Purpose**
1	Achromatic doublet lens	1	Edmund Optics (#63-714)	127.20	Objective lens
2	3mm ball lens	1	Edmund Optics (#43-711)	25.97	Objective lens
3	Plano-convex lens	1	Holmarc Opto-Mechatronics Ltd.	8.70	Tube lens
4	Aspherical compound lens (Reversed)	1	Amazon/local electronics market	4.28	Relay or coupling lens
5	Emission filter	1	Edmund Optics (#67-016)	267.78	Fluorescence signal filter
6	LED	3	RS Components	<1.5	Illumination source
7	ESP32 development board with micro USB cable	1	Amazon/local electronics market	10.18	Illumination control
8	Smartphone USB-OTG	1	Amazon/local electronics market	<1.99	Serial communication and powering
9	Wires	—	Amazon/local electronics market	<0.1	Connection
10	Screw and spring	1 each	Local market	<0.1	For focusing mechanism in 3D-printed translational stage
11	3D-printed embodiments	—	Designed and fabricated in the laboratory	<1	Holding of opto-electronics components

4.4 Summary

In summary, the first section of the present chapter demonstrates the working of a low-cost, field-portable smartphone optical microscope which has been developed using 3D printed technology and off-the-shelf optical components. The designed microscopic system has the optical resolution well below 2.0 μm. By using the cloud-based application, the imaging quality of the microscopic images has been enhanced. Use of cloud-based services ensures the minimal use of smartphone hardware including RAM, CPU, GPU and storage elements which is crucial for the low-end devices. BF and fluorescence modes of imaging are the most important and widely used instruments in research laboratories and biomedical applications. In the second section of the chapter, the optimization in the optical configuration of a $4f$ imaging setup has been investigated and extended the platform for BF and fluorescence imaging on a single platform. The designed tool has been developed using commonly available optical components, 3D-printed modules, and optoelectronics parts. The figures of merit of the system have been experimentally characterized. The lateral resolution of the designed platform is estimated to be 1.21 μm. The system is not only suitable for statistical studies of the cells but also useful to study the morphological applications. Three different magnification levels 1.16×, 2.86× and 37.33× are supported by this imaging platform. The versatility and capability of the system has been demonstrated through morphological and statistical studies of blood cells.

Present work highlighted the working of the device that operates in BF and single-color fluorescence mode of imaging. It is worth mentioning here that the device is also capable of imaging in DF, polarized and multi-color fluorescence modalities by incorporating suitable optical components such as filters, polarizer-analyzer and LEDs. These studies will be carried out in the future course of works.

References

[1] Ballard, Z. S., Brown, C., and Ozcan, A. Mobile technologies for the discovery, analysis, and engineering of the global microbiome. *ACS nano*, 12(4):3065–3082, 2018.

[2] Zhang, W., Guo, S., Carvalho, W. S. P., Jiang, Y., and Serpe, M. J. Portable point-of-care diagnostic devices. *Analytical Methods*, 8(44):7847–7867, 2016.

[3] Liu, J., Geng, Z., Fan, Z., Liu, J., and Chen, H. Point-of-care testing based on smartphone: The current state-of-the-art (2017–2018). *Biosensors and Bioelectronics*, 132:17–37, 2019.

[4] Vashist, S. K., Luppa, P. B., Yeo, L. Y., Ozcan, A., and Luong, J. H. Emerging technologies for next-generation point-of-care testing. *Trends in biotechnology*, 33(11):692–705, 2015.

[5] Breslauer, D. N., Maamari, R. N., Switz, N. A., Lam, W. A., and Fletcher, D. A. Mobile phone based clinical microscopy for global health applications. *PloS one*, 4(7):e6320, 2009.

[6] Zeng, Y., Jin, K., Li, J., Liu, J., Li, J., Li, T., and Li, S. A low cost and portable smartphone microscopic device for cell counting. *Sensors and Actuators A: Physical*, 274:57–63, 2018.

[7] Huang, X., Xu, D., Chen, J., Liu, J., Li, Y., Song, J., Ma, X., and Guo, J. Smartphone-based analytical biosensors. *Analyst*, 143(22):5339–5351, 2018.

[8] Jung, D., Choi, J.-H., Kim, S., Ryu, S., Lee, W., Lee, J.-S., and Joo, C. Smartphone-based multi-contrast microscope using color-multiplexed illumination. *Scientific reports*, 7(1):1–10, 2017.

[9] Gross, H. *Handbook of Optical Systems, Volume 1, Fundamentals of Technical Optics*, volume 1. 2005.

[10] Diederich, B., Lachmann, R., Carlstedt, S., Marsikova, B., Wang, H., Uwurukundo, X., Mosig, A. S., and Heintzmann, R. A versatile and customizable low-cost 3d-printed open standard for microscopic imaging. *Nature communications*, 11(1):1–9, 2020.

[11] Hergemöller, T. and Laumann, D. Smartphone magnification attachment: microscope or magnifying glass. *The Physics Teacher*, 55(6):361–364, 2017.

[12] Wang, Z., Bovik, A. C., Sheikh, H. R., and Simoncelli, E. P. Image quality assessment: from error visibility to structural similarity. *IEEE transactions on image processing*, 13(4):600–612, 2004.

[13] Sara, U., Akter, M., and Uddin, M. S. Image quality assessment through fsim, ssim, mse and psnr—a comparative study. *Journal of Computer and Communications*, 7(3):8–18, 2019.

[14] Ozcan, A. Mobile phones democratize and cultivate next-generation imaging, diagnostics and measurement tools. *Lab on a Chip*, 14(17):3187–3194, 2014.

[15] Antony, P. P. M. A., Trefois, C., Stojanovic, A., Baumuratov, A. S., and Kozak, K. Light microscopy applications in systems biology: opportunities and challenges. *Cell Communication and Signaling*, 11(1):1–19, 2013.

[16] Ji, N. Adaptive optical fluorescence microscopy. *Nature methods*, 14(4):374–380, 2017.

[17] Contreras-Naranjo, J. C., Wei, Q., and Ozcan, A. Mobile phone-based microscopy, sensing, and diagnostics. *IEEE Journal of Selected Topics in Quantum Electronics*, 22(3):1–14, 2015.

[18] Switz, N. A., D'Ambrosio, M. V., and Fletcher, D. A. Low-cost mobile phone microscopy with a reversed mobile phone camera lens. *PloS one*, 9(5):e95330, 2014.

[19] Zhu, W., Pirovano, G., O'Neal, P. K., Gong, C., Kulkarni, N., Nguyen, C. D., Brand, C., Reiner, T., and Kang, D. Smartphone epifluorescence microscopy for cellular imaging of fresh tissue in low-resource settings. *Biomedical optics express*, 11(1):89–98, 2020.

[20] Wong, C., Pawlowski, M. E., Forcucci, A., Majors, C. E., Richards-Kortum, R., and Tkaczyk, T. S. Development of a universal, tunable, miniature fluorescence microscope for use at the point of care. *Biomedical Optics Express*, 9(3):1041–1056, 2018.

[21] Agbana, T. E., Diehl, J.-C., van Pul, F., Khan, S. M., Patlan, V., Verhaegen, M., and Vdovin, G. Imaging & identification of malaria parasites using cellphone microscope with a ball lens. *PloS one*, 13(10):e0205020, 2018.

[22] Zhu, H., Sencan, I., Wong, J., Dimitrov, S., Tseng, D., Nagashima, K., and Ozcan, A. Cost-effective and rapid blood analysis on a cell-phone. *Lab on a Chip*, 13(7):1282–1288, 2013.

[23] Gao, T., Smith, Z. J., Lin, T.-y., Carrade Holt, D., Lane, S. M., Matthews, D. L., Dwyre, D. M., Hood, J., and Wachsmann-Hogiu, S. Smart and fast blood counting of trace volumes of body fluids from various mammalian species using a compact, custom-built microscope cytometer. *Analytical chemistry*, 87(23): 11854–11862, 2015.